Bulletin of the Chemical Society of Japan, 2025, **98**, uoaf048
https://doi.org/10.1093/bulcsj/uoaf048
Advance access publication 13 June 2025

Award Accounts

Structural selection rules in self-assembly and self-organization: role of entropy production rate

Hideki Nabika*

Faculty of Science, Yamagata University, 1-4-12 Kojirakawa, Yamagata 990-8560, Japan

*Corresponding author: Faculty of Science, Yamagata University, 1-4-12 Kojirakawa, Yamagata 990-8560, Japan. Email: nabika@sci.kj.yamagata-u.ac.jp

Hideki Nabika
Hideki Nabika received his PhD from Kobe University in 2004 under the supervision of Professor Shigehito Deki. He joined the research group of Professor Kei Murakoshi at Hokkaido University as an assistant professor in 2003 and moved to Yamagata University as an associate professor in 2011. In 2014, he was promoted to the post of professor at Yamagata University. His research interests are the self-assembly and self-organization for both artificial and living systems. His recent research explores how the entropy production rate governs structural selection, aimed at exploring common thermodynamic principles underlying both self-assembly and self-organization.

Abstract

Self-assembly and self-organization are mechanisms by which ordered structures are formed spontaneously in nature. Traditionally, these phenomena have been distinguished thermodynamically: self-assembly occurs via free energy minimization toward equilibrium, whereas self-organization occurs in open systems maintained far from equilibrium via continuous energy dissipation. Despite this contrast, both processes involve dynamic pathways governed by entropy production during structure formation. Recent findings have shown that the entropy production rate is important in determining the selection rule for the resultant structure. Herein, we first summarize the differences and similarities between self-assembly and self-organization, along with representative examples, from micelles and crystals to convective flows and chemical oscillations. Then, we focus on the entropy production rate as a principle governing structure selection during non-equilibrium processes in both self-assembly and self-organization regimes. Our recent experimental findings reveal how flux conditions influence structure selection in reaction–diffusion systems (Liesegang phenomenon) and protein self-assembly. This perspective suggests that nature, including biological systems, may selectively harness self-assembly or self-organization depending on the interplay between energy flux and the kinetics of the involved reactions. These insights highlight the potential of an entropy-based analysis to enhance our understanding of complex pattern formation and guide the rational design of self-assembly and self-organization.

Keywords: entropy production rate, self-assembly, self-organization.

Graphical Abstract

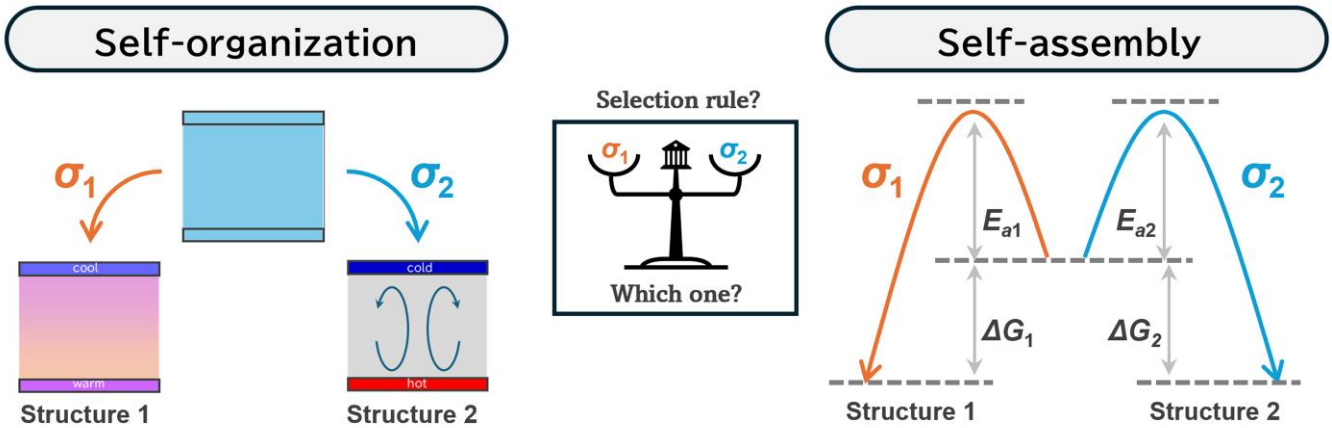

[Received on 9 May 2025; revised on 23 May 2025; accepted on 23 May 2025; corrected and typeset on 13 June 2025]

1. The central role of self-assembly and self-organization in nature

Atoms, ions, molecules, particles, and even biological entities like cells can spontaneously form structures with temporal or spatial order. Based on their thermodynamics, these processes are broadly categorized as self-assembly or self-organization.[1–7] Such self-assembly and self-organizing behavior are fundamental to the development of structure and function in natural system. Because of their relevance in different fields across chemistry, physics, biology, and materials science, these processes have attracted considerable research attention. While self-assembly is typically associated with systems approaching thermodynamic equilibrium, self-organization occurs in open systems maintained far from equilibrium. Despite these differences, both processes involve spontaneous structure formation via non-equilibrium pathways. Highlighting their fundamental and cross-disciplinary importance, the journal *Science* commemorated its 125th anniversary with a special issue titled "What Don't We Know?", which presented 125 of the most compelling unsolved scientific questions.[8] Alongside grand questions, such as "Why do humans have so few genes?",[9] "Can the laws of physics be unified?",[10] and "Are we alone in the universe?",[11] a key chemistry-related question appeared: "How Far Can We Push Chemical Self-Assembly?".[12] This inclusion strongly implies the importance of self-assembly as a core science, raising the possibility that chemists may someday emulate, or even exceed, nature's capabilities in designing complex self-assembly and self-organization processes.

1.1 Thermodynamic design principles of self-assembly

Typical examples of self-assembled structures, such as crystals and micelles (Fig. 1a), can be rationalized based on thermodynamic principles (Fig. 1b). Specifically, molecular assembly occurs when the assembled state is energetically more stable than the dispersed one. In good solvents, the dispersed state

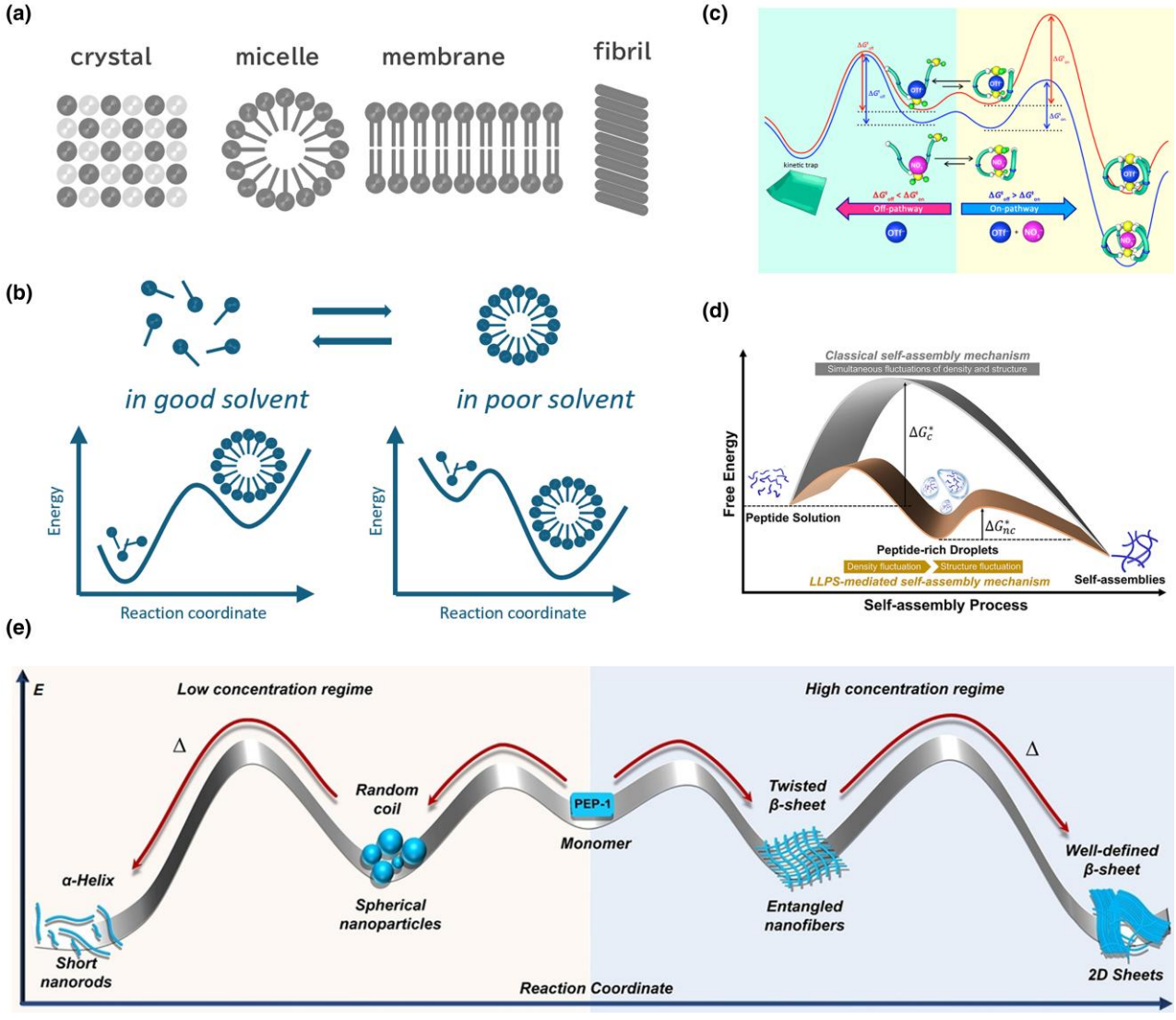

Fig. 1. Thermodynamic principles for molecular self-assembly. a) Typical examples of self-assembly, which proceed when the assembled state is more favorable than the non-assembled one, which is illustrated in (b). c) Control of molecular interactions as a pathway selector: kinetic template effects govern the assembly morphology.[13] d) Influence of the surrounding environment: peptide-mediated phase separation enables control of the self-assembly pathway. Reprinted with permission of Elsevier.[16] e) Influence of internal molecular conformation: increased concentration of protein building blocks drives transitions from amorphous aggregates to ordered β-sheet structures.[17]

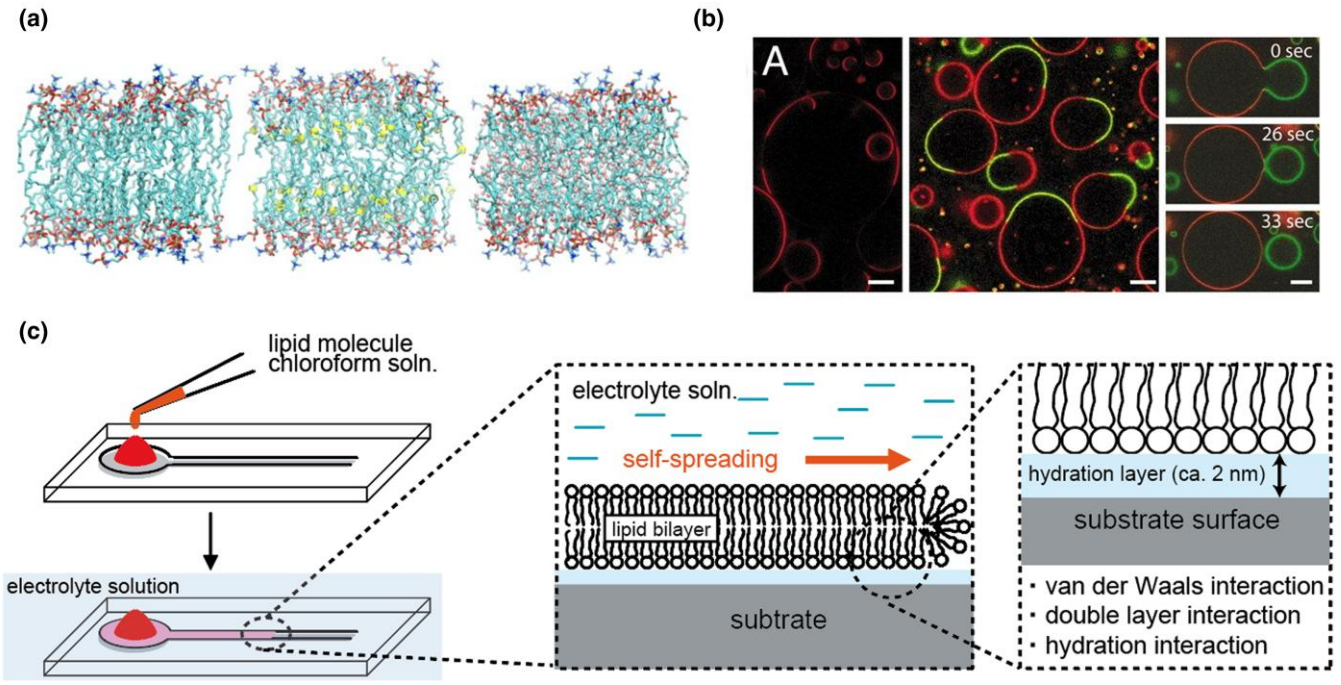

Fig. 2. Thermodynamically driven self-assembly in lipid membrane systems. a) Spontaneous formation of lipid bilayers in aqueous media due to amphiphilic character. Reprinted with permission of Elsevier.[26] b) Phase separation in model membranes resulting in coexisting liquid-ordered and liquid-disordered domains, relevant to biological lipid rafts. Copyright (2005) National Academy of Sciences, USA.[22] c) Self-spreading of lipid bilayers at a water–lipid–solid interface: transition from a metastable disordered aggregate to an ordered membrane under hydration. Reprinted with permission of Elsevier.[23]

is energetically more stable and assembly does not occur. In contrast, in poor solvents, assembly becomes thermodynamically favorable and thus proceeds spontaneously, capturing the behavior implied by the prefix "self" in self-assembly. This intrinsic simplicity implies that, in principle, chemists can control self-assembly via rational molecular and thermodynamic design. For example, Fig. 1c demonstrates the control of the energy landscape for self-assembling pathways by the kinetic template effect, which demonstrates how direct control over intermolecular interactions can determine self-assembly pathways.[13] While this example highlights how chemists can tune the energy landscape in terms of molecular aspects, it is increasingly evident that the physicochemical properties of the surrounding environment are also important in controlling the energy landscape. In biological systems, phase separation has emerged as a key mechanism for developing dynamic and membraneless compartments that regulate a wide range of cellular functions.[14,15] As such, biological systems occasionally utilize phase separation to design the energy landscape (Fig. 1d).[16] While phase separation illustrates how the surrounding environment can reshape the energetic landscape, the intrinsic properties of the assembled molecules themselves also play a critical role in modulating self-assembly. This is especially relevant in biological macromolecules like proteins, in which secondary structure formation can shift the balance between disordered and ordered states. Figure 1e presents a representative example, in which conformational transitions act as an additional design parameter influencing the resulting morphology. In this case, increasing the concentration of protein-derived building blocks was found to shift the equilibrium from amorphous aggregates to well-defined β-sheet structures, thereby demonstrating how hierarchical control over molecular conformation influences thermodynamic stability.[17]

These examples collectively illustrate that self-assembly is a fundamental principle regulating both structural architectures and functional behaviors in biological systems. Among the most fundamental biological instances of self-assembly is the formation of lipid bilayers, which serve as the structural basis of cellular membranes (Fig. 2a).[18–22] These bilayers are formed spontaneously in aqueous environments due to the amphiphilic nature of lipids. Importantly, thermodynamic stabilization does not always lead to uniformity; instead, it can promote the formation of spatial heterogeneity via phase separation. For example, model lipid membranes composed of simple binary or ternary mixtures have been known to exhibit liquid–liquid phase separation into coexisting liquid-ordered and liquid-disordered domains; this effect is considered relevant to biological phenomena like lipid rafts (Fig. 2b).[23] They exhibit lateral heterogeneity, asymmetric composition, and dynamic remodeling, all of which suggest that cells have evolved mechanisms for the precise regulation of self-assembled architecture for functional purposes. Another example of how lipids undergo self-assembly under thermodynamic guidance is the self-spreading phenomenon, which is the spontaneous growth of a lipid bilayer at a water–lipid–solid interface (Fig. 2c).[24–30] In this system, a disordered lipid aggregate deposited on a dry solid substrate is thermodynamically unfavorable. Upon hydration, it reorganizes into an ordered planar lipid membrane. This transition reflects a spontaneous movement toward thermodynamic equilibrium, driven by the free energy minimization of both lipid–lipid and lipid–substrate interactions.

Such observations confirm that self-assembly can proceed spontaneously, without active control, under the guidance of energy landscape, spanning a wide range of systems from

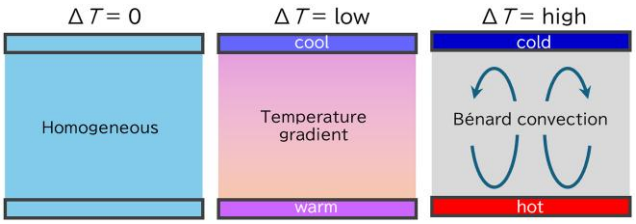

Fig. 3. Thermal convection as a model of self-organization in open systems. (left) At equilibrium, no temperature gradient exists in a stationary glass of water. (middle) Heating from below introduces a temperature gradient, resulting in a non-equilibrium steady state with conductive heat transfer. (right) Further heating induces Rayleigh–Bénard convection rolls, forming a dissipative structure that enhances entropy production.

small species like ions and ligands to large biomacromolecules like lipids and proteins.

1.2 Self-organization in non-equilibrium systems

While self-assembly proceeds toward thermodynamic equilibrium under the influence of intermolecular forces, self-organization refers to the emergence of ordered structures in systems that are maintained far from equilibrium (non-equilibrium). A clear example of self-organization with energy dissipation is the behavior of water in a glass (Fig. 3). At equilibrium, a glass of water left undisturbed in a room will eventually reach a homogeneous temperature matching its surroundings. In this state, there is no net energy flow (dissipation), no temperature gradient, and no macroscopic structure (right panel in Fig. 3). The system is thermodynamically stable and no further apparent changes occur. However, if the glass is heated from below (middle panel in Fig. 3), a temperature gradient begins to form, where the bottom becomes warmer than the top. Although this configuration appears unstable in terms of uniformity, it represents a non-equilibrium steady state in which continuous energy dissipation through thermal conduction stabilizes the system. Thus, the state with a temperature gradient can remain stationary. As the bottom temperature increases further (right panel in Fig. 3), a critical threshold is reached where thermal diffusion alone can no longer efficiently dissipate the incoming energy. At this point, the system undergoes a transition and spontaneously develops convective rolls, known as Rayleigh–Bénard convection, which enhance energy dissipation through bulk fluid motion compared with the temperature gradient. If the heating continues and evaporation is negligible, the convective state itself becomes stationary, which is also a non-equilibrium steady state supported by constant energy dissipation. These structures such as water in glass with a temperature gradient and constant convective flow exemplify a dissipative structure, which is a concept introduced by Ilya Prigogine to describe how order can arise and persist with an energy dissipation in open systems driven far from equilibrium.

In the cases shown in Fig. 3, heat serves as the input energy that sustains the structures formed as non-equilibrium steady states. If this concept is applied to chemical reaction systems, the input of energy can be replaced by the chemical potential of the reaction substrates to maintain continuous reactions. A typical example is the Belousov–Zhabotinsky (BZ) reaction. In a continuously stirred tank reactor (CSTR), the BZ reaction generates striking oscillations in the concentrations of chemical components in the system (Fig. 4a).[31] These collective oscillations form a temporally ordered structure maintained by the constant flux of substrate and products. In this system, the chemical substrates act as the energy source, while the associated reaction heat and products are continuously dissipated into the environment. As long as the substrate is continuously supplied and reaction proceeds, energy dissipation persists and the dynamic oscillatory behavior is stabilized as a non-equilibrium steady state. The oscillatory dynamics of the BZ reaction stem from nonlinear chemical kinetics, particularly autocatalytic steps that introduce positive feedback. This feedback amplifies fluctuations, enabling sustained oscillations and complex spatiotemporal patterns. This concept has been extended to construct a class of pH oscillators, where the proton concentration is regulated through autocatalytic feedback (Fig. 4b).[32–36] These systems demonstrated that oscillations can be engineered by embedding suitable kinetic motifs. Remarkably, this conceptual framework has been realized in synthetic biochemical systems. For example, a DNA-based reaction network reproduces predator–prey-type oscillations through designed strand displacement reactions and catalytic amplification steps (Fig. 4c).[37] These examples collectively highlight the universality of autocatalytic nonlinearity as a design principle for constructing oscillatory chemical systems, both in classical inorganic reactions and in synthetic molecular networks.

In addition to temporal oscillations, self-organization in non-equilibrium systems frequently gives rise to spatial pattern formation.[41,42] For example, the BZ reaction can form concentric rings or spiral wave patterns that propagate across the medium (Fig. 4d).[38] Another class of spatial self-organization is Turing patterns (Fig. 4e),[39,43–45] in which reaction–diffusion systems spontaneously develop stationary and periodic structures. An intriguing manifestation of self-organization at the interface between chemical and mechanical phenomena is shown in Fig. 4f, where droplets containing the chemical substrates for the BZ reaction can exhibit spontaneous and periodic oscillations in their propulsion speed.[40] In this system, the internal redox oscillations of the BZ reaction drive dynamic changes in interfacial tension, which in turn modulate the Marangoni flow responsible for droplet motion. This coupling between chemical oscillations and mechanical responses enables a form of chemomechanical feedback, where temporal self-organization at the molecular level manifests as periodic modulation of macroscopic behavior. Such systems represent a novel class of dissipative structures in which reaction–diffusion dynamics and mechanical motion are intrinsically linked, offering unique platforms for exploring active matter and autonomous chemical machines.

Taken together, these examples demonstrate how self-organization can emerge spontaneously under continuous energy dissipation, manifesting in diverse systems ranging from thermal fluids to chemical oscillators, unified by the principles of non-equilibrium dynamics.

2. Entropy production and structure selection: from self-assembly to self-organization

While self-assembly such as crystallization or lipid bilayer formation produces structures where the repeating units are of similar size to the constituent molecules, self-organization under non-equilibrium conditions, such as in the BZ reaction or Rayleigh–Bénard convection, gives rise to spatial patterns

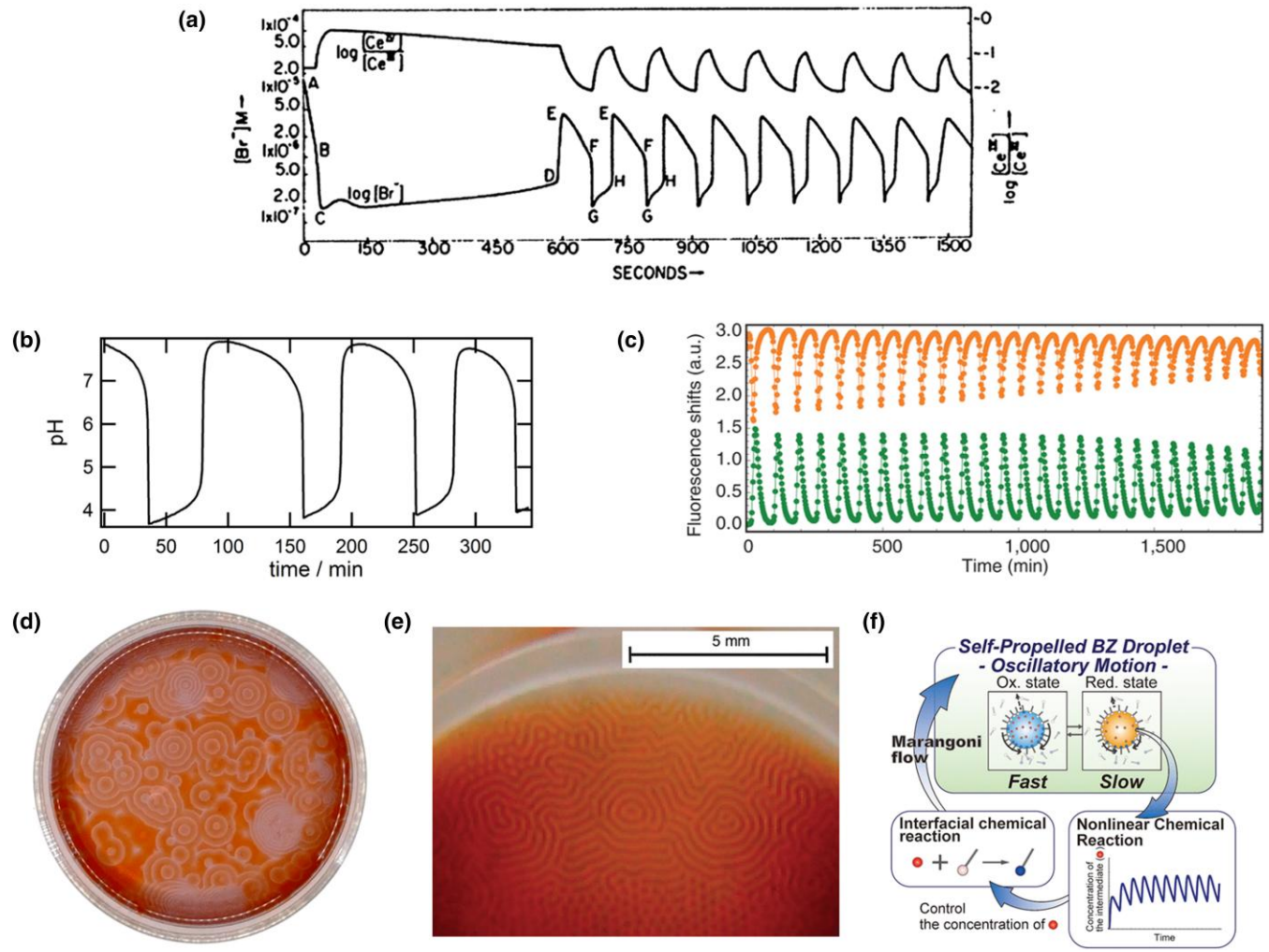

Fig. 4. Temporal and spatial self-organization in chemical systems. a) Temporal oscillations in BZ reaction within a CSTR: redox states alternate periodically due to nonlinear autocatalytic reactions. Reprinted with permission from ref. [31]. Copyright (1972) American Chemical Society. b) pH oscillator as a synthetic autocatalytic reaction system generating periodic proton fluctuations. Reproduced with permission of Elsevier.[36] c) DNA-based synthetic oscillator mimicking predator–prey dynamics via strand displacement and catalytic amplification. Reprinted with permission from ref [37]. Copyright (2013) American Chemical Society. d) Concentric or spiral wave patterns of BZ reaction in a thin layer, illustrating spatial patterning.[38] e) Stationary periodic Turing patterns from reaction–diffusion systems via local activation and long-range inhibition. Reprinted with permission from ref. [39]. Copyright (2011) American Chemical Society. f) Chemomechanical coupling in a self-propelled BZ droplet: redox oscillations modulate interfacial tension and droplet motion. Reprinted with permission from ref. [40]. Copyright (2016) American Chemical Society.

with characteristic wavelengths that far exceed the size of the individual components. This distinction reflects a fundamental difference in the principles governing order formation: thermodynamic minimization in equilibrium versus sustained energy dissipation in open systems. This thermodynamic distinction is further clarified by considering entropy production. In self-assembly, the system spontaneously evolves toward a state of minimum free energy, generating entropy during the course of assembly. However, it eventually reaches thermodynamic equilibrium, where entropy production ceases and no further apparent change occurs. In contrast, self-organization takes place in open systems with a continuous entropy production due to sustained energy flow, which maintains temporal or spatial order by the ongoing energy dissipation. Such behavior has been quantitatively demonstrated in systems like thermal convection, where convective states are shown to exhibit higher entropy production rates.[46,47] As shown in Fig. 5a, the *y*-component of the local thermodynamic fluxes (J) for the axially symmetric flow

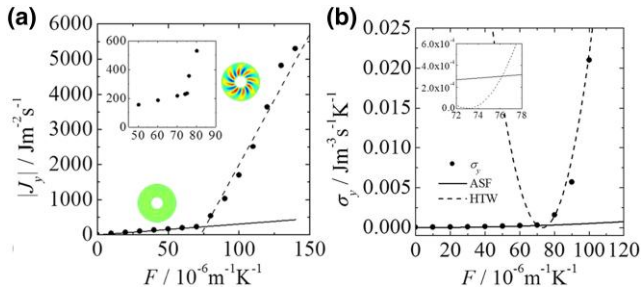

Fig. 5. Entropy production as a structure selection principle. a) Local thermodynamic fluxes in thermal convection systems (ASF vs. HTW) show distinct linear regimes versus driving force F.[47] b) Corresponding entropy production shows a discontinuous transition between ASF and HTW states.[47]

(ASF) and hydrothermal wave (HTW) states exhibits two distinct linear regimes with respect to the driving force F. This leads to a discontinuous transition in the *y*-component of

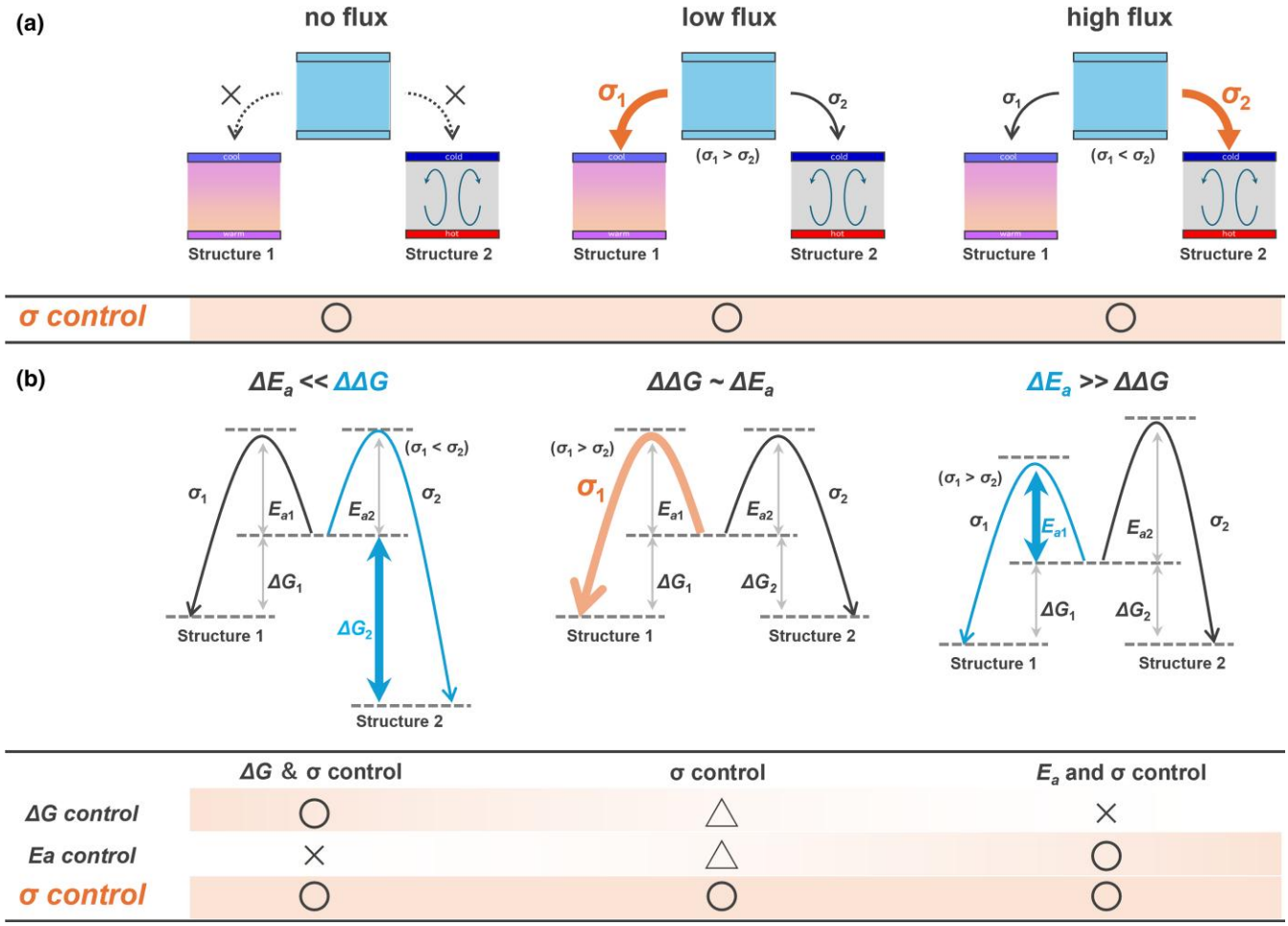

Fig. 6. Flux-dependent selection of macroscopic structures. a) The structure selection in self-organization, where the structural transitions between a conductive state (Structure 1: temperature gradient) and a convective state (Structure 2: Bénard convection) under increasing heat flux is illustrated. With increasing flux, the system shifts its state from the stationary state to the temperature gradient (structure 1) and then to convective flow (structure 2), which is rationalized by larger entropy production. b) The energy diagrams of self-assembly, emphasizing how structural selection shifts from thermodynamically favored (left) to kinetically favored (right) pathways, depending on the magnitude of the free energy gain and activation energy. However, NH_4Cl selects the self-assembled structure that yields higher σ, depending on the degree of supersaturation. If $\sigma_1 > \sigma_2$, the self-assembly proceeds toward Structure 1 (middle).

entropy production (σ) at a critical value of F, as illustrated in Fig. 5b. The result indicates that the transition between ASF and HTW is governed by a selection of the state with higher σ, providing direct evidence for entropy-driven structural selection in thermal convection. This finding supports the idea that entropy production plays a decisive role in structural selection under non-equilibrium conditions. The tendency of natural systems to evolve structures and states with the largest entropy production is captured by the concept of the maximum entropy production principle (MEPP).[48,49]

This principle is conceptually summarized in Fig. 6a for the system shown in Fig. 3 as a model case. When no thermal input (left), the system cannot dissipate the energy and σ is zero. Thus, water is stationary and the apparent structure does not evolve. When low flux is added (middle), the system adopts a stable state with a temperature gradient without macroscopic motion (referred to as Structure 1) because σ is higher than that for the state with Rayleigh–Bénard convection (Structure 2), i.e. $\sigma_1 > \sigma_2$. However, as the flux increases further (right), the entropy production rates are reversed ($\sigma_1 < \sigma_2$), leading the system to transition into the convective state. This sequence of transitions, from stationary to the temperature gradient and then to convective flow, demonstrates that the system spontaneously selects the state and structure with the highest σ under each condition. This indicates that σ serves as a key factor in controlling the structure and state of the system under an open system with energy dissipation.

The σ value not only acts as a controlling parameter for selecting the dissipative structures in self-organization but may also enable structure selection during self-assembly. A typical example is provided by the growth behavior of ammonium chloride (NH_4Cl) crystals.[50] During crystallization under varying supersaturation conditions, NH_4Cl dendrites underwent a transition in growth orientation: at lower supersaturation, the crystals preferentially grew along the ⟨1 0 0⟩ direction, while at higher supersaturation, growth shifted to the ⟨1 1 0⟩ and ⟨1 1 1⟩ axes.[50] This change in morphology suggests that the system selects different self-assembly directions depending on the degree of supersaturation. Such behavior can be rationalized within the same framework observed during self-organization, i.e. MEPP, where the structure associated with higher σ is more likely to be selected. Actually, the transition observed in the growth direction corresponds to a

shift toward morphologies with greater σ during the crystallization.[51] Although crystallization will finally reach thermodynamic equilibrium without further apparent changes, this finding strongly indicates that the non-equilibrium process during crystallization is controlled by the magnitude of σ. Thus, this example shows the possibility that MEPP can act as the structure selection rule to explain and predict the structures formed by self-assembly, like self-organization.

However, the transition in the growth direction of NH_4Cl based on σ cannot be explained in terms of classical thermodynamic or kinetic control as shown in Fig. 1. Notably, however, the concept of σ-based control inherently includes both thermodynamic and kinetic frameworks. To clarify this issue, three plausible structure selection rules observed in the self-assembly processes are compared in Fig. 6b. In the left panel of Fig. 6b, the system represents a case with a large free energy difference ($\Delta\Delta G$) between the two structures, while the difference in activation energy (ΔE_a) is small. In such systems, the structure with the greater free energy gain (Structure 2) is selected, indicating thermodynamic control. This is a natural outcome, as Structure 2 is more stable ($\Delta G_2 > \Delta G_1$), and the activation energy barriers are nearly identical ($E_{a1} \approx E_{a2}$). Importantly, the structural selection in this case cannot be predicted reasonably based on the activation energy alone. In contrast, the right panel of Fig. 6b illustrates a system in which the free energy difference ($\Delta\Delta G$) is small, while the activation energy difference (ΔE_a) is large. In this scenario, the structure with the lower activation barrier (Structure 1) is selected, indicating that the structural selection was governed primarily by kinetic control. In other words, selection in this system cannot be explained by ΔG. Together, these two contrasting examples demonstrate that the dominant factor governing structural selection depends on the relative magnitudes of ΔG and E_a.

Let us now revisit why ΔG and E_a act as criteria for selecting reaction pathways involved in self-assembly. Thermodynamic selection based on ΔG (left panel in Fig. 6b) focuses on the amount of heat that can be released during a reaction, while kinetic selection based on activation energy E_a (right panel in Fig. 6b) emphasizes how fast a reaction can proceed. These two viewpoints, heat generation and reaction rate, are inherently linked to σ, which is proportional to the amount of reaction per unit time and the heat produced per reaction event. In this light, a system that selects pathways with larger ΔG (left panel) can be reinterpreted as favoring reactions that produce more entropy per reaction event. Similarly, a system that favors reactions with lower Ea can be used to select faster pathways that contribute to greater entropy production over time. Further, even when ΔG and E_a are almost the same and the reaction pathway cannot be determined from either ΔG or E_a (middle panel in Fig. 6b), the preferred structure can still be identified as the one with the highest σ. If entropy production rates (σ_1, σ_2) are visualized as the thickness of the curved arrows, and if $\sigma_1 > \sigma_2$, then the selection of Structure 1 becomes consistent with MEPP (the middle panel in Fig. 6b). Therefore, while structure selection based on ΔG or E_a is applicable only under specific energetic conditions, the σ-based method is a more universal one applicable across a wide range of self-assembling systems, regardless of whether thermodynamic or kinetic considerations alone are sufficient. In this sense, the concept of σ-based control would not only encompass but also integrate the classical thermodynamic and kinetic frameworks into a single and cohesive principle for understanding structure selection during self-assembly.

These findings suggest that σ may serve as a common organizing principle underlying both self-organization and self-assembly, the latter of which proceeds via non-equilibrium pathways during structure formation. From crystallization to dissipative pattern formation, the principle of selecting structures with higher σ appears to operate across a wide range of systems. Yet, a fully unified theoretical framework that considers these phenomena along a continuous spectrum of entropy-producing processes has yet to be established. To move closer to such a framework, experimental efforts that deliberately probe intermediate regimes, where equilibrium and non-equilibrium characteristics coexist, are especially valuable because they provide critical insights into how σ governs structure selection across different thermodynamic landscapes for both self-organization and self-assembly.

3. Flux-driven structure selection: experimental case studies

In this review, we explore two experimental techniques for studying self-assembly and self-organization, focusing on how the thermodynamic driving force (the degree of supersaturation) governs structure selection. The first case is the Liesegang phenomenon, a classical pattern formation protocol driven by the interplay between molecular diffusion and nonlinear chemical reactions under supersaturated conditions. The second case involves the self-assembly of proteins in biological systems. While protein self-assembly has traditionally been discussed in terms of equilibrium structures, the intracellular environment is fundamentally an open and dissipative energy-consuming system. This raises a critical question: can the in vivo self-assembly of proteins, occurring under non-equilibrium and dissipative conditions, truly be equated with protein behavior in closed, equilibrium systems? In this review, we discuss our recent efforts to address this unresolved issue by developing experimental models examining how entropy production governs self-assembly and self-organization, both of which proceed via non-equilibrium processes with entropy production, using supersaturation as the experimentally tunable driving force.

3.1 Liesegang pattern formation under controlled flux

As discussed above, one example of structure selection governed by MEPP is the growth orientation of NH_4Cl crystals, where the crystallization direction depends on supersaturation.[50,51] While past studies have focused on homogeneous aqueous systems, a more complex class of phenomena arises when anisotropic diffusion and crystal formation occur cooperatively in reaction–diffusion systems such as the Liesegang phenomenon.[52]

The Liesegang phenomenon refers to the periodic precipitation patterns when an electrolyte A is homogeneously incorporated in a gel matrix, and another electrolyte B is allowed to diffuse into it from one side (Fig. 7a).[53–57] During the diffusion of B into the gel matrix containing A, the formation of insoluble salts (AB) proceeds from the interface between the gel and solution, when the solubility product [A][B] in the gel phase exceeds the corresponding solubility product (K_{sp}). Thus, most experiments on the Liesegang phenomenon have been limited to systems that use sparingly soluble salts. Under appropriate conditions, the precipitation of sparingly soluble salt AB does not proceed homogeneously in space,

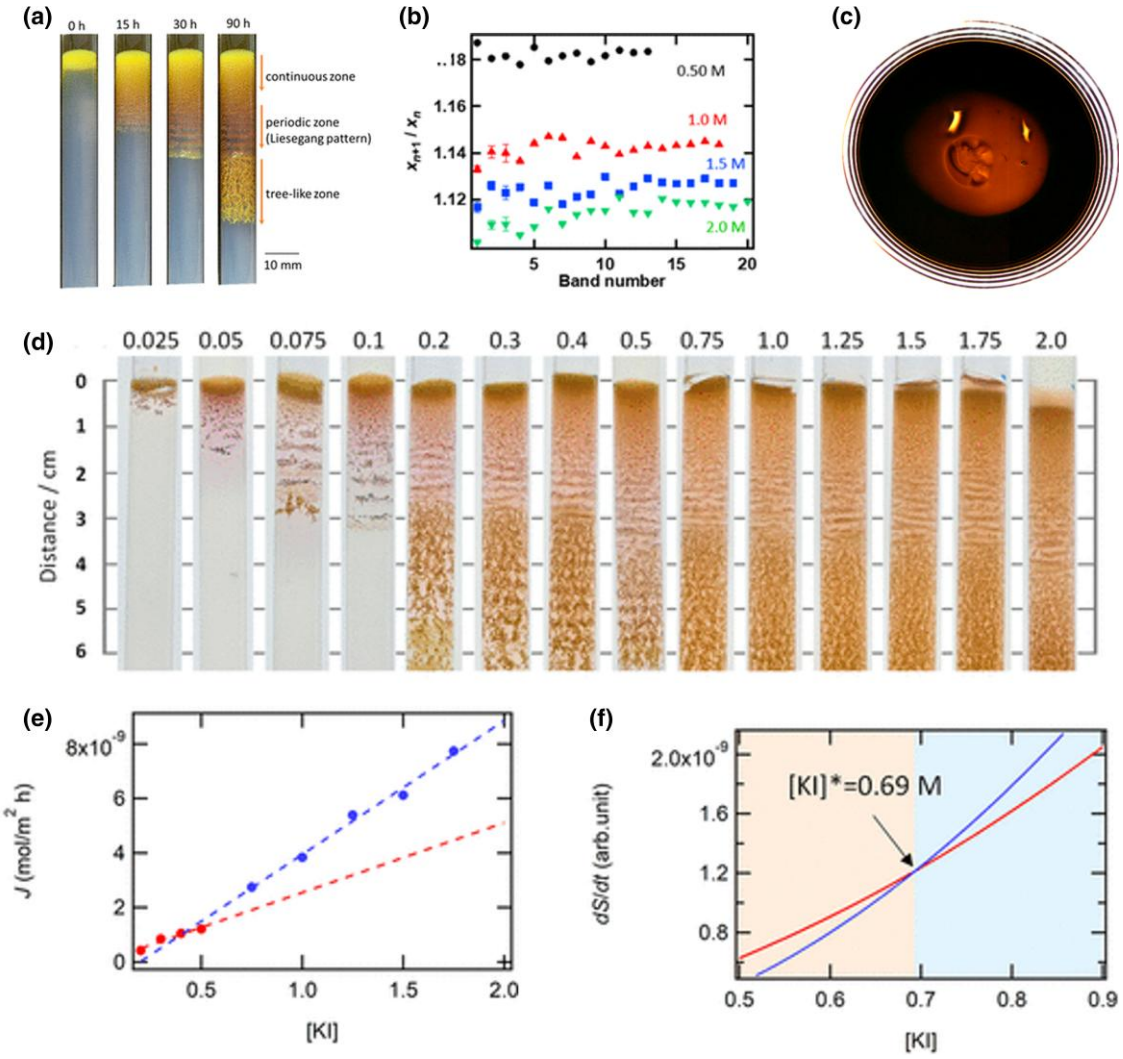

Fig. 7. MEPP-based structure selection in Liesegang pattern formation. a) Schematic of Liesegang pattern formation: diffusion of outer electrolyte into a gel containing inner electrolyte yields continuous, periodic, and tree-like precipitation of the corresponding insoluble salt. Reprinted with permission from ref. [54]. Copyright (2022) American Chemical Society. b) Periodic precipitation bands formed under appropriate conditions, which obeys the spacing law. Reprinted with permission from ref. [53]. Copyright (2021) American Chemical Society. c) Liesegang-type patterning via metal ion reduction without explicit solubility thresholds. Reprinted with permission from ref. [57]. Copyright (2022) American Chemical Society. d) Morphological transition in dendritic crystal growth as a function of supersaturation (external [KI]). Reprinted with permission from ref. [54]. Copyright (2022) American Chemical Society. e) Thermodynamic flux vs. external electrolyte concentration shows two distinct linear regimes. Reprinted with permission from ref. [54]. Copyright (2022) American Chemical Society. f) Entropy production rates cross at critical concentration (~0.69 M), coinciding with symmetry transition in dendritic structures. Reprinted with permission from ref. [54]. Copyright (2022) American Chemical Society.

but yields a series of discrete bands with geometric spacing. This empirical periodicity, known as the spacing law (Fig. 7b), is derived from the nonlinear nature of the precipitation reaction between two electrolytes. In classical systems, this nonlinearity is typically associated with a concentration threshold defined by K_{sp}, indicating that pattern formation is limited to reactions governed by K_{sp}, i.e. salt-formation reactions. However, Liesegang patterns were found to form in systems without an explicit concentration threshold K_{sp}. For example, we have succeeded in the formation of Liesegang patterns from the reduction reactions of metal ions, where there is no concentration threshold to proceed with the reaction (Fig. 7c).[58–60] In this system, numerical simulation showed that the concentration threshold for the nucleation step introduces an effective nonlinearity and is also the origin of the formation of the periodic structure.[59] Since the nucleation process is common to many chemical reactions involving solid formation, this study is significant in that its finding shows that the Liesegang phenomenon is not limited to sparingly soluble salts, but can also occur in any system where solids are formed.

Recent studies have shown that MEPP-based structure selection is also operative in such Liesegang systems.[55] Specifically, when the concentration of the inner electrolyte $Pb(NO_3)_2$ within the gel is held constant at 1.0×10^{-2} M and the concentration of the outer electrolyte KI in the upper solution is systematically varied from 0.025 to 2.0 M, the dendritic crystals formed beneath the discrete precipitation bands exhibit a symmetry transition at around 0.75 M (Fig. 7d). At lower concentrations (e.g.$\leq$0.5 M), the dendritic structures display horizontal periodicity, consistent with the above Liesegang bands. In contrast, at higher concentrations (e.g. $\geq$1.0 M), orientation changes to the vertical direction, which is a well-known feature of dendrites. To investigate the

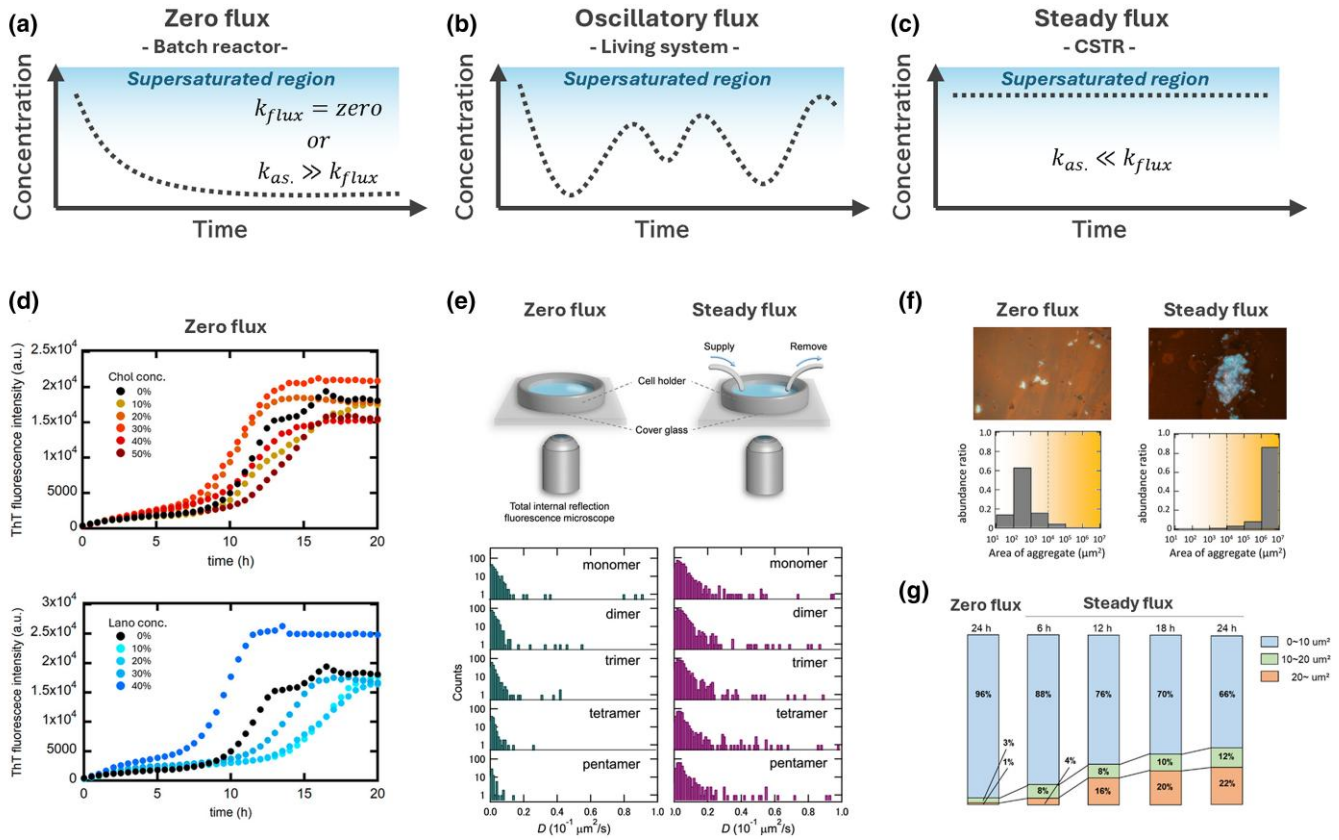

Fig. 8. Influence of flux on protein self-assembly dynamics and structure. a) Zero-flux regime: substrate is consumed over time, leading to equilibrium (batch reactor-like behavior). b) Oscillatory-flux regime: biologically relevant time-varying flux as seen in circadian rhythms and CSF flow. c) Steady-flux regime: constant influx and efflux maintain stable substrate levels (CSTR). d) Most in vitro studies of protein self-assembly are performed under zero-flux conditions and observe the reach at the equilibrium state. Reprinted with permission from ref. [61]. Copyright (2025) American Chemical Society. e) Upper: Experimental setups for steady flux: sample solution cells with micro-pump. Lower: There are some amyloid-β oligomers with higher lateral diffusivities under the steady-flux condition. Reprinted with permission from ref. [62]. Copyright (2025) American Chemical Society. f, g) Under steady flux, amyloid-β assemblies grow larger and exhibit higher compared to zero-flux conditions. Reprinted with permission from ref. [63]. Copyright (2021) American Chemical Society.

thermodynamic basis of this transition, the thermodynamic flux J was estimated from the crystal growth velocity and plotted as a function of the outer electrolyte concentration, corresponding to the degree of supersaturation and the driving force for crystal formation. The results showed two distinct linear regimes for lower and higher KI concentrations (Fig. 7e), similar to those observed for thermal convection systems (Fig. 5). Calculations of entropy production rates for each regime revealed that the dominant structure at any given concentration coincides with the one exhibiting higher entropy production (Fig. 7f). Notably, a crossover in entropy production occurs at approximately 0.69 M, closely matching the critical concentration that changes the orientation of the dendrites. These findings provide suggest that even in reaction–diffusion systems, the formation of macroscopic periodic structures is governed by entropy production. Importantly, this result extends the validity of MEPP from simple crystallization in homogeneous solutions to systems with increased physicochemical complexity.

It should be noted, however, that unlike dissipative structures like thermal convection,[46,47] Liesegang patterns form via non-equilibrium processes, but the formed periodic structures are subsequently fixed by the gel matrix even without flux. This indicates that the Liesegang patterns are not dissipative in nature under non-equilibrium steady states. Nevertheless, the observation of MEPP-driven transitions in this reaction–diffusion system highlights its value as an intermediate between fully dissipative structures (e.g. thermal convection) and fully equilibrium self-assembly (e.g. NH_4Cl crystal growth).

3.2 Protein self-assembly under controlled flux

As demonstrated in the above examples, the degree of supersaturation can control the structure of self-assembly and self-organization. Although the degree of supersaturation changes with the progress of the self-assembly and self-organization, its temporal behavior depends on whether the system is closed or open. In closed systems with zero flux, the degree of supersaturation (i.e. the concentration of reaction substrates) decreases monotonically as the assembly proceeds. This finally leads to an equilibrium state where the concentration becomes constant and no further apparent structural change occurs (Fig. 8a). Similarly, even in systems with non-zero flux, if the rate of flux k_{flux} is significantly lower than the intrinsic rate of self-assembly $k_{\mathrm{association}}$, the system behaves similar to the closed system with zero flux. In both cases, the system tends toward a static endpoint governed by equilibrium thermodynamics, which is typical of batch reactors. In the steady-flux regime, substrates are continuously supplied to the system at

a constant rate. This configuration corresponds to a CSTR, a widely used setup in chemical engineering to maintain the chemical process in the reactor. When k_{flux} is sufficiently higher than $k_{association}$, the substrate concentration remains constant over time (Fig. 8c). Both zero-flux and steady-flux regimes represent well-established boundary conditions in classical chemical systems, such as batch and flow reactors.

However, biological environments often exhibit dynamic fluctuations in mass flux due to intrinsic rhythmic or physiological cycles. One such example is the circadian fluctuation observed in cerebrospinal fluid (CSF) flow, whose flow rate can vary by a factor of 20 between waking and sleeping conditions,[64] implying that the k_{flux} in the brain undergoes significant temporal modulation. Such fluctuations result in an oscillatory-flux regime, wherein the substrate concentration in the system is driven by periodic changes in flux regulated by biological rhythms (Fig. 8b). This condition is neither strictly closed nor constant-flowing, but rather exemplifies a biologically relevant, time-dependent control of self-organization.

As illustrated in Fig. 8a–c, the classification of a system as closed or open depends on the relative magnitudes of k_{flux} and $k_{association}$. For small molecules such as water, self-assembly typically occurs on the nanosecond timescale,[65] which is far faster than the timescale of biological rhythms. In such cases, even if a flux exists, the overall process can be well approximated by a monotonic decrease in substrate concentration, as observed in closed systems (Fig. 8a). In contrast, the self-assembly of biological macromolecules, such as proteins with high flexibility, often proceeds on timescales of several hours.[61,63] This duration is occasionally comparable to the time scale of fluctuations driven by biological rhythms. Despite this, most experimental studies on protein self-assembly have been conducted under closed, equilibrium-oriented conditions without considering substrate flux (Fig. 8d).[63]

This raises a fundamental question: Should we continue investigating protein self-assembly under closed-system conditions (Fig. 8a), or should we adopt open-system frameworks like those in Fig. 8b and c that account for realistic biological fluxes? To address this question, we conducted a comparative study of protein self-assembly under two well-defined flux regimes: a zero-flux condition, in which no external substrate supply was introduced, and a steady-flux condition, in which biologically relevant levels of substrate flux were maintained. Using the same protein in both cases, we investigated how the presence or absence of flux alters the structural selection.

To experimentally investigate the impact of flux on protein self-assembly, we constructed two distinct steady-flux systems: a microfluidic channel[62] and a solution cell coupled with a micro-pump (Fig. 8e).[66] In both systems, a solution of monomeric amyloid-β (Aβ) peptides was continuously delivered over several days to maintain a constant flux, thereby simulating a biologically relevant steady-state environment. In the microfluidic experiments, the presence of steady-flux afforded significantly larger assemblies than those produced under the zero-flux condition (Fig. 8f).[62] Under zero flux, the average assembly size remained around 10 μm^2 after 24 h. In contrast, under steady-flux conditions, assembly growth persisted throughout the observation period, and after 24 h, more than 20% of the structures exceeded 20 μm^2 in area. These results suggest that the rate of self-assembly is increased substantially under steady flux, likely due to the sustained supersaturation maintained in the system, as conceptually compared in Fig. 8a and c.

Steady flux was also found to accelerate the formation of oligomeric intermediates, which is the initial step toward larger assemblies.[66] Furthermore a clear difference was observed between the nature of the oligomers formed under zero flux and those formed under steady flux. For example, the oligomers formed under steady flux exhibited higher lateral diffusivity on supported lipid membranes than those formed under zero flux (Fig. 8e lower panel), implying flux-dependent variations in oligomer structure or the membrane-oligomer interaction. These findings indicate that steady flux could alter the kinetics as well as the structure selection of protein self-assembly. While enhanced kinetics can simply be explained by the continuous sustainment of supersaturation, the physical basis for the differences in diffusivity in the membrane remains unclear. However, by analogy with previous studies on NH_4Cl crystallization and Liesegang pattern formation, where distinct flux conditions afforded morphologically distinct structures governed by MEPP, the differing flux regimes in our experiments may be thought to afford distinct entropy production rates, potentially influencing the selection of self-assembled structures in protein systems.

This structure selection demonstrated that substrate flux critically influences protein self-assembly. Under steady-flux conditions, amyloid-β assemblies grew larger and exhibited altered diffusive properties compared to those formed under zero flux. These differences suggest that continuous supersaturation enhances assembly kinetics and also modulates the structural states of oligomers. Drawing parallels with MEPP-governed systems like NH_4Cl crystallization and Liesegang patterns, the results obtained in this study can suggest the possibility that flux-dependent entropy production rate may similarly guide structure selection in biological macromolecular self-assemblies.

4. Summary and outlook

In this review, we have examined the distinction between self-assembly and self-organization from a thermodynamic perspective. Traditionally, these processes have been differentiated in terms of their relationship to energy flow: self-assembly is viewed as a pathway toward energy minimization in closed systems, while self-organization occurs in open systems maintained by continuous energy dissipation. However, this clear distinction overlooks the fact that even self-assembly involves entropy production during structure formation before reaching equilibrium. When both processes are examined in terms of entropy production rate, a potential unifying principle begins to emerge. In particular, MEPP may provide a common framework for understanding structural selection in both the equilibrium and non-equilibrium regimes. This perspective is supported by experimental findings across a range of systems, including crystal growth of NH_4Cl, thermal convection, Liesegang pattern formation, and protein self-assembly, each demonstrating that structure selection in both self-assembly and self-organization can be governed by entropy production rates.

Returning to the question posed by Science in its 125th anniversary, "How Far Can We Push Chemical Self-Assembly?", we believe that the examples and discussions presented in this review represent a possible step toward answering this question. By elucidating how thermodynamic driving forces and

the entropy production rate govern the non-equilibrium processes underlying both self-assembly and self-organization, we hope to contribute to a unified framework for understanding molecular organization in both artificial systems and complex living systems. Thus, we aim to bridge the gap between classical chemical models and the dynamic complexity of life.

Acknowledgments

I express my deepest gratitude to the many individuals who supported and inspired me throughout my academic journey and in the research activities that led to this commemorative review. I am especially grateful to Prof. Shigehito Deki, Prof. Minoru Mizuhata, Dr. Akihiko Kajinami, and Prof. Kensuke Akamatsu (Konan University), who supported me throughout my studies at Kobe University and shaped my early development as a scientist. I would also like to express my sincere appreciation to Prof. Kei Murakoshi of Hokkaido University, under whose supervision I served as an assistant professor. During this time, I not only enhanced my expertise in physical chemistry but also rediscovered the importance of scientific integrity, perseverance, and intellectual curiosity in research. His guidance has greatly influenced my approach to conducting and thinking about science, and I remain deeply thankful for the formative impact he had on my academic development. After joining Yamagata University and starting my independent research as a principal investigator, I made a significant shift into the field of self-organization in non-equilibrium and nonlinear systems, which is the subject recognized by this award. I have been fortunate to work with and be supported by many outstanding researchers in this field. In particular, I would like to thank Prof. Satoshi Nakata (Hiroshima University), Prof. Takashi Amemiya (Yokohama National University), Prof. Koichi Asakura (Keio University), Dr. Takahiko Ban (Osaka University), Prof. Takahiro Nakamura (Meiji University), Prof. Qing Fang (Yamagata University), Prof. Hiroyuki Kitahata (Chiba University), Prof. Nobuhiko J. Suematsu (Meiji University), Dr. Yoshiko Takenaka (AIST), Dr. Yusuke Hara (AIST), and Dr. Taisuke Banno (Keio University). Their collaboration, discussion, and encouragement have played a vital role in the progress of my work. I am especially grateful to Prof. S. Nakata, for his invaluable support in broadening my research activities in the field of non-equilibrium self-organization. I also extend my sincere thanks to Dr. T. Ban for his insightful discussions on the maximum entropy production principle (MEPP), which forms a central theme of this review, as well as for his valuable suggestions regarding future research directions. Special thanks are owed to the students of the author's laboratory at Yamagata University, with whom the core body of research featured in this commemorative review was conducted. Their dedication, creativity, and tireless efforts made possible the experimental advances and insights discussed herein. In particular, Dr. Masaki Itatani (Hokkaido University) and Dr. Yusuke Inomata (Kumamoto University) are gratefully acknowledged for their outstanding contributions.

Funding

The authors gratefully acknowledge the financial support from JSPS KAKENHI (Grant Nos. 08034429, 08103828, 10011790, 25708012, 26520203, 26600021, 16H04092, 18K19051, 19H02668, and 23K23294); The Japan Science Society; the Akiyama Life Science Foundation; Research Foundation for Opto-Science and Technology; Tokuyama Science Foundation; The Ebara Hatakeyama Memorial Foundation; The Hitachi Global Foundation; The Kao Foundation for Arts and Sciences; The Foundation for Japanese Chemical Research; The Asahi Glass Foundation; Intelligent Cosmos Academic Foundation; Nippon Sheet Glass Foundation for Materials Science and Engineering; Yamaguchi Educational and Scholarship Foundation; Takeda Science Foundation; Sumitomo Electric Group CSR Foundation; Harmonic Ito Foundation; Asahi Group Foundation.

Conflict of interest statement. None declared.

Data availability

This paper was prepared under an Award Account, and no experimental data are available for disclosure.

References

1. B. Grzybowski, C. Wilmer, J. Kim, K. Browne, K. Bishop, *Soft Matter* **2009**, *5*, 1110. https://doi.org/10.1039/b819321p
2. K. Ariga, X. Jia, J. Song, J. P. Hill, D. T. Leong, Y. Jia, J. Li, *Angew. Chem. Int. Ed. Engl.* **2020**, *59*, 15424. https://doi.org/10.1002/anie.202000802
3. B. A. Grzybowski, K. J. M. Bishop, C. J. Campbell, M. Fialkowski, S. K. Smoukov, *Soft Matter* **2005**, *1*, 114. https://doi.org/10.1039/b501769f
4. A.-D. C. Nguindjel, P. J. de Visser, M. Winkens, P. A. Korevaar, *Phys. Chem. Chem. Phys.* **2022**, *24*, 23980. https://doi.org/10.1039/D2CP02542F
5. I. R. Epstein, B. Xu, *Nat. Nanotechnol.* **2016**, *11*, 312. https://doi.org/10.1038/nnano.2016.41
6. E. Nakouzi, O. Steinbock, *Sci. Adv.* **2016**, *2*, e1601144. https://doi.org/10.1126/sciadv.1601144
7. *Self-organized Motion: Physicochemical Design Based on Nonlinear Dynamics*, ed. by Satoshi Nakata, Veronique Pimienta, Istvan Lagzi, Hiroyuki Kitahata, Nobuhiko J. Suematsu, Royal Society of Chemistry, Cambridge, England, **2018**.
8. D. Kennedy, C. Norman, *Science* **2005**, *309*, 75. https://doi.org/10.1126/science.309.5731.75
9. E. Pennisi, *Science* **2005**, *309*, 80. https://doi.org/10.1126/science.309.5731.80
10. C. Seife, *Science* **2005**, *309*, 82. https://doi.org/10.1126/science.309.5731.82
11. R. A. Kerr, *Science* **2005**, *309*, 88. https://doi.org/10.1126/science.309.5731.88
12. R. F. Service, *Science* **2005**, *309*, 95. https://doi.org/10.1126/science.309.5731.95
13. L. H. Foianesi-Takeshige, S. Takahashi, T. Tateishi, R. Sekine, A. Okazawa, W. Zhu, T. Kojima, K. Harano, E. Nakamura, H. Sato, S. Hiraoka, *Commun. Chem.* **2019**, *2*, 1. https://doi.org/10.1038/s42004-019-0232-2
14. A. A. Hyman, C. A. Weber, F. Jülicher, *Annu. Rev. Cell Dev. Biol.* **2014**, *30*, 39. https://doi.org/10.1146/annurev-cellbio-100913-013325
15. R. Kobayashi, H. Nabika, *Soft Matter* **2024**, *20*, 5331. https://doi.org/10.1039/D4SM00470A
16. C. Yuan, Q. Li, R. Xing, J. Li, X. Yan, *Chem* **2023**, *9*, 2425. https://doi.org/10.1016/j.chempr.2023.05.009
17. G. Ghosh, R. Barman, A. Mukherjee, U. Ghosh, S. Ghosh, G. Fernández, *Angew. Chem. Int. Ed. Engl.* **2022**, *61*, e202113403. https://doi.org/10.1002/anie.202113403

18. J. N. Israelachvili, D. J. Mitchell, B. W. Ninham, *Biochim. Biophys. Acta* **1977**, *470*, 185. https://doi.org/10.1016/0005-2736(77)90099-2
19. M. Antonietti, S. Förster, *Adv. Mater.* **2003**, *15*, 1323. https://doi.org/10.1002/adma.200300010
20. T. Kunitake, Y. Okahata, *J. Am. Chem. Soc.* **1977**, *99*, 3860. https://doi.org/10.1021/ja00453a066
21. T. Harayama, H. Riezman, *Nat. Rev. Mol. Cell Biol.* **2018**, *19*, 281. https://doi.org/10.1038/nrm.2017.138
22. X. Zhuang, J. R. Makover, W. Im, J. B. Klauda, *Biochim. Biophys. Acta* **2014**, *1838*, 2520. https://doi.org/10.1016/j.bbamem.2014.06.010
23. K. Bacia, P. Schwille, T. Kurzchalia, *Proc. Natl. Acad. Sci. U. S. A.* **2005**, *102*, 3272. https://doi.org/10.1073/pnas.0408215102
24. J. Raedler, H. Strey, E. Sackmann, *Langmuir* **1995**, *11*, 4539. https://doi.org/10.1021/la00011a058
25. H. Nabika, B. Takimoto, K. Murakoshi, *Anal. Bioanal. Chem.* **2008**, *391*, 2497. https://doi.org/10.1007/s00216-008-2140-7
26. H. Nabika, A. Fukasawa, K. Murakoshi, *Phys. Chem. Chem. Phys.* **2008**, *10*, 2243. https://doi.org/10.1039/b715983h
27. H. Nabika, A. Fukasawa, K. Murakoshi, *Langmuir* **2006**, *22*, 10927. https://doi.org/10.1021/la062459y
28. H. Nabika, A. Sasaki, B. Takimoto, Y. Sawai, S. He, K. Murakoshi, *J. Am. Chem. Soc.* **2005**, *127*, 16786. https://doi.org/10.1021/ja0559597
29. K. Furukawa, K. Sumitomo, H. Nakashima, Y. Kashimura, K. Torimitsu, *Langmuir* **2007**, *23*, 367. https://doi.org/10.1021/la062911d
30. F. Tamura, Y. Tanimoto, R. Nagai, F. Hayashi, K. Morigaki, *Langmuir* **2019**, *35*, 14696. https://doi.org/10.1021/acs.langmuir.9b02685
31. R. J. Field, E. Koros, R. M. Noyes, *J. Am. Chem. Soc.* **1972**, *94*, 8649. https://doi.org/10.1021/ja00780a001
32. G. Rabai, M. Orban, I. R. Epstein, *Acc. Chem. Res.* **1990**, *23*, 258. https://doi.org/10.1021/ar00176a004
33. M. Orbán, K. Kurin-Csörgei, I. R. Epstein, *Acc. Chem. Res.* **2015**, *48*, 593. https://doi.org/10.1021/ar5004237
34. H. Nabika, Y. Inumata, T. Oikawa, K. Unoura, *Chem. Lett.* **2012**, *41*, 1139. https://doi.org/10.1246/cl.2012.1139
35. H. Nabika, T. Oikawa, K. Iwasaki, K. Murakoshi, K. Unoura, *J. Phys. Chem. C. Nanomater. Interfaces* **2012**, *116*, 6153. https://doi.org/10.1021/jp300650c
36. H. Nabika, T. Inumata, H. Kitahata, K. Unoura, *Colloids Surf. A. Physicochem. Eng. Asp.* **2014**, *460*, 236. https://doi.org/10.1016/j.colsurfa.2014.04.014
37. T. Fujii, Y. Rondelez, *ACS Nano* **2013**, *7*, 27. https://doi.org/10.1021/nn3043572
38. L. Howell, E. Osborne, A. Franklin, É Hébrard, *J. Phys. Chem. B* **2021**, *125*, 1667. https://doi.org/10.1021/acs.jpcb.0c11079
39. K. Asakura, R. Konishi, T. Nakatani, T. Nakano, M. Kamata, *J. Phys. Chem. B* **2011**, *115*, 3959. https://doi.org/10.1021/jp111584u
40. N. J. Suematsu, Y. Mori, T. Amemiya, S. Nakata, *J. Phys. Chem. Lett.* **2016**, *7*, 3424. https://doi.org/10.1021/acs.jpclett.6b01539
41. I. R. Epstein, K. Showalter, *J. Phys. Chem.* **1996**, *100*, 13132. https://doi.org/10.1021/jp953547m
42. P. K. Maini, K. J. Painter, H. N. P. Chau, *J. Chem. Soc., Faraday Trans.* **1997**, *93*, 3601. https://doi.org/10.1039/a702602a
43. S. Kondo, T. Miura, *Science* **2010**, *329*, 1616. https://doi.org/10.1126/science.1179047
44. J. Howard, S. W. Grill, J. S. Bois, *Nat. Rev. Mol. Cell Biol.* **2011**, *12*, 392. https://doi.org/10.1038/nrm3120
45. S. Kondo, R. Asal, *Nature* **1995**, *376*, 765. https://doi.org/10.1038/376765a0
46. T. Ban, *Entropy* **2020**, *22*, 800. https://doi.org/10.3390/e22080800
47. T. Ban, K. Shigeta, *Sci. Rep.* **2019**, *9*, 10368. https://doi.org/10.1038/s41598-019-46921-2
48. L. M. Martyushev, V. D. Seleznev, *Phys. Rep.* **2006**, *426*, 1. https://doi.org/10.1016/j.physrep.2005.12.001
49. L. M. Martyushev, *J. Exp. Theor. Phys.* **2007**, *104*, 651. https://doi.org/10.1134/S1063776107040152
50. S.-K. Chan, H.-H. Reimer, M. Kahlweit, *J. Cryst. Growth* **1976**, *32*, 303. https://doi.org/10.1016/0022-0248(76)90111-1
51. A. Hill, *Nature* **1990**, *348*, 426. https://doi.org/10.1038/348426a0
52. H. Nabika, M. Itatani, I. Lagzi, *Langmuir* **2020**, *36*, 481. https://doi.org/10.1021/acs.langmuir.9b03018
53. M. Itatani, Q. Fang, K. Unoura, H. Nabika, *J. Phys. Chem. B* **2020**, *124*, 8402. https://doi.org/10.1021/acs.jpcb.0c05603
54. M. Itatani, Q. Fang, H. Nabika, *J. Phys. Chem. B* **2021**, *125*, 6921. https://doi.org/10.1021/acs.jpcb.1c02175
55. H. Nabika, K. Tsukada, M. Itatani, T. Ban, *Langmuir* **2022**, *38*, 11330. https://doi.org/10.1021/acs.langmuir.2c01602
56. K. Tsushima, M. Itatani, Q. Fang, H. Nabika, *Langmuir* **2023**, *39*, 249. https://doi.org/10.1021/acs.langmuir.2c02441
57. Y. Yatsuda, K. Tsushima, Q. Fang, H. Nabika, *ACS Earth Space Chem.* **2023**, *7*, 2042. https://doi.org/10.1021/acsearthspacechem.3c00165
58. H. Nabika, M. Sato, K. Unoura, *Langmuir* **2014**, *30*, 5047. https://doi.org/10.1021/la5003786
59. M. Itatani, Q. Fang, K. Unoura, H. Nabika, *J. Phys. Chem. C. Nanomater. Interfaces* **2018**, *122*, 3669. https://doi.org/10.1021/acs.jpcc.7b12688
60. M. Matsue, M. Itatani, Q. Fang, Y. Shimizu, K. Unoura, H. Nabika, *Langmuir* **2018**, *34*, 11188. https://doi.org/10.1021/acs.langmuir.8b02335
61. J. Habchi, S. Chia, C. Galvagnion, T. C. T. Michaels, M. M. J. Bellaiche, F. S. Ruggeri, M. Sanguanini, I. Idini, J. R. Kumita, E. Sparr, S. Linse, C. M. Dobson, T. P. J. Knowles, M. Vendruscolo, *Nat. Chem.* **2018**, *10*, 673. https://doi.org/10.1038/s41557-018-0031-x
62. A. Iida, M. Abe, M. Nochi, C. Soga, K. Unoura, H. Nabika, *J. Phys. Chem. Lett.* **2021**, *12*, 4453. https://doi.org/10.1021/acs.jpclett.1c00524
63. K. Akiho, A. Iida-Adachi, H. Nabika, *ACS Chem. Neurosci.* **2025**, *16*, 195. https://doi.org/10.1021/acschemneuro.4c00707
64. L. Xie, H. Kang, Q. Xu, M. J. Chen, Y. Liao, M. Thiyagarajan, J. O'Donnell, D. J. Christensen, C. Nicholson, J. J. Iliff, T. Takano, R. Deane, M. Nedergaard, *Science* **2013**, *342*, 373. https://doi.org/10.1126/science.1241224
65. M. Matsumoto, S. Saito, I. Ohmine, *Nature* **2002**, *416*, 409. https://doi.org/10.1038/416409a
66. A. Iida-Adachi, H. Nabika, *Langmuir* **2025**, *41*, 3121. https://doi.org/10.1021/acs.langmuir.4c03663